Scientia Iranica B (2014) 21(1), 192–202

SCIENTIA IRANICA

Sharif University of Technology
Scientia Iranica
Transactions B: Mechanical Engineering
www.scientiairanica.com

The unsteady behavior of subsonic wind tunnel wall pressure during pitching motion of the model

A.R. Davari[*,a], **M.R. Soltani**[b] **and M. Ghaeminasab**[a]

a. *Department of Mechanical and Aerospace Engineering, Islamic Azad University, Science and Research Branch, Poonak, Tehran, P.O. Box: 14155-4933, Iran.*
b. *Department of Aerospace Engineering, Sharif University of Technology, Tehran, P.O. Box: 11155-9567, Iran.*

Received 5 September 2012; received in revised form 10 March 2013; accepted 9 September 2013

KEYWORDS
Interference effect; Pitching oscillation; Reduced frequency; Disturbance convection.

Abstract. Extensive low speed wind tunnel experiments have been undertaken to measure the test section, floor wall pressure distribution, in the presence of a 2D wing inside the test section. The experiments were performed for both the static and dynamic pitching motion of the model under different conditions. In these measurements, the effects of the existence and oscillations of a 2D wing on the floor wall pressure at various locations were studied. According to the results, as the oscillation parameters, such as mean angle of attack and frequency, change, wall pressures at the points located in the front part of the test section, in the upstream region, exhibit different behavior from those in the downstream. Viscosity is shown to be a major contributor in convecting fluctuations, caused by model oscillations, to the flowfield. As the Reynolds number increases, the downstream region receives fewer disturbances from the pure dynamic motion of the model. It is believed that static wake is the dominant contributor, in the absence of viscous effects.

1. Introduction

The proximity of test section walls to the model surface is expected to affect the flowfield in such a way that measured parameters cannot be extended to those in practice. This interference problem between the model and wind tunnel walls can be even more complicated when the model oscillates inside the test section. In contrast to static wind tunnel testing, where extensive calibrations are commonly used to account for wall interference on aerodynamic characteristics, in dynamic tests, there is a complicated coupling between the unsteady support and wall interference mechanisms, and conventional aerodynamic testing knowledge is not likely to account for these interference effects [1].

At high angles of attack, the vortices or the wake shed from the model interact with the walls. In addition, any flow separation in the diffuser or on the walls downstream of the model can create an unsteady pressure gradient, which will affect the pressure field on the model, as well as transverse acoustic interference [2]. These communications between the model and the surrounding wall have been extensively investigated.

There were a number of tests conducted in the 1980s, at NASA, which comprehensively characterize the effect of wind tunnel walls on unsteady airfoil motion [3-5]. In addition, a theoretical work by Fromme and Goldberg sheds a lot of light on this topic [5,6]. These investigations are concerned with the impact of a solid wall and its distance on the steady and unsteady aerodynamic behavior of the airfoil. Ahmed et al. [7] also studied flow characteristics over an airfoil with moving ground simulations and at different ground clearances. They found a strong

*. *Corresponding author.*
E-mail addresses: ardavari@srbiau.ac.ir (A.R. Davari); msoltani@sharif.edu (M.R. Soltani); mghaemi@yahoo.com (M. Ghaeminasab)

relationship between the ground clearance at different angles of attack and the aerodynamic behavior of the airfoil.

Duraisamy et al. [8] studied the effect of wall interference on steady and oscillating airfoils in a subsonic wind tunnel. They examined a variety of approaches, including linear theory and compressible inviscid and viscous computations, as well as experimental data, to study the aforementioned phenomena.

In steady flow, their results showed augmentation of lift magnitude when the wall is close to the airfoil surface. For oscillating airfoils, lift augmentation was accompanied by a significant change in the phase of the lift response.

Ericsson and Beyers [9] reviewed the existing extensive experimental data base for delta wings to explain wall and support system interference effects on the leading edge vortices of delta wings. They found that Reynolds number scaling, wind tunnel wall interference and model support interference place conflicting requirements on the test parameters. The discrepancies between the results are significantly reduced when taking these phenomena into account.

The attempts made so far have mainly been concentrated on wall effects on the steady and unsteady aerodynamic behavior of the model. This information, while being valuable, still lacks details about the convection mechanism of disturbances from the model to the flowfield, the way the disturbances propagate and the parameters responsible for this propagation.

These details can be used in the model design phase for a wind tunnel test to reduce adverse wall interference effects. Also, in such practical applications as a helicopter in ground effect, wind turbines, hovercrafts, etc., where the ground effect is a part of reality and must not be eliminated from the problem, this information is helpful in the design and analysis processes.

In this paper, a new aspect of the subsonic model-wall interference problem has been introduced. Wind tunnel wall pressure fluctuations at different streamwise locations were measured, while a 2D model was oscillating inside the test section. The results, expressed in the form of a power spectrum and hysteresis loops, give some information about the way an oscillating model communicates with a flowfield, both upstream and downstream, and the parameters affecting it.

Note that this study was part of ongoing experimental research into a wind turbine blade, and several aerodynamic aspects of these blade sections have already been studied by Soltani et al. [10], Soltani and Birjandi [11], Soltani and Rasi [12] and Soltani et al. [13].

2. Experimental setup and procedure

The experiments were performed in a subsonic wind tunnel. The tunnel is of a closed return type and has a test section dimension of 80×80 cm^2. The maximum attainable speed in the test section is 100 m/sec. According to hot wire measurements, the turbulence intensity in the test section is less than 0.1%.

The investigations have been performed on the floor wall of the test section to study the effects of model oscillation on wall pressure distribution. The model was a 2D wing with the geometric characteristics of a 660 kW wind turbine blade. Figure 1 shows the model installed in the test section. Twelve small equally spaced holes were carefully drilled into the lower wall of the test section, each connecting to a sensitive pressure transducer. Figure 2 shows the pressure tab arrangement on the floor, along with the geometric details of the airfoil. The tab locations were distributed from upstream to almost far downstream of the model, each having 1 mm diameter. Five pressure tabs were provided downstream of the model in the wake region, two points exactly under the model, near the leading and trailing edges, respectively, and five points upstream of the model, all located streamwise in a line midway between the left and right side walls. The pressure tabs were connected to the transducers located outside the test section by plastic tubes. According to the studies of Soltani et al. [14], tube length and material were chosen in such a manner that the associated pressure losses and time lags are at a minimum.

In the mechanism used for oscillating the model, the rotational motion of an electric motor was converted through a crank shaft, joints and connecting

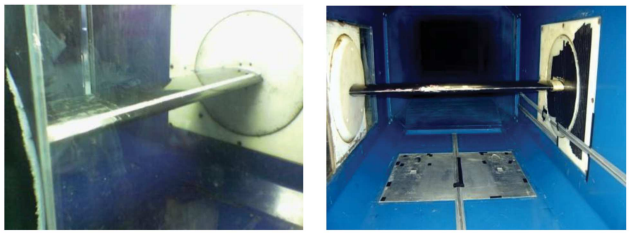

Figure 1. The 2D wing model installed in the test section.

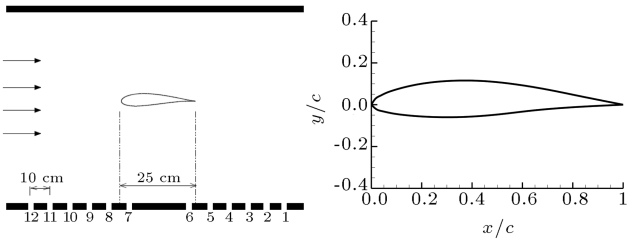

Figure 2. Airfoil geometry and schematic view of pressure tabs locations.

rods, into the reciprocating motion. The pivot point in the present experiments was at the quarter chord of the wing, and the oscillation frequency was controlled by the motor RPM. The oscillation amplitude could be varied by adjusting the joints and the connecting rods.

The tests were conducted at two constant free stream velocities corresponding to the Reynolds number of 5.0×10^5 and 10.0×10^5, based on the chord length. The model was set at two different mean angles of attack, 5 and 18 degrees, and was oscillated at various frequencies. The floor static pressure distribution was recorded during the model oscillations inside the test section. All data were acquired by AT-MIO-64E-3 data acquisition board capable of scanning 64 channels at a maximum rate of 500 KHz.

An analytical approach [15,16] was also used to estimate the errors encountered in the pressure measurements. Both the single sample precision and the bias uncertainty in the pressure measurement were estimated. On this basis, the overall uncertainty for the presented data is less than $\pm\%3$.

3. Results and discussion

The experiments were performed for both static and dynamic pitching motions for various mean angles of attack and pitching frequencies. In the dynamic tests, the pitching amplitudes were $\pm5^\circ$ and $\pm18^\circ$. The static, followed by the dynamic, results are presented in the following sections.

3.1. Static results

In Figure 3, the static pressure distribution on the bottom wall of the test section has been presented, while the model was set to various angles of attack. For low to moderate angles of attack, a gentle recovery

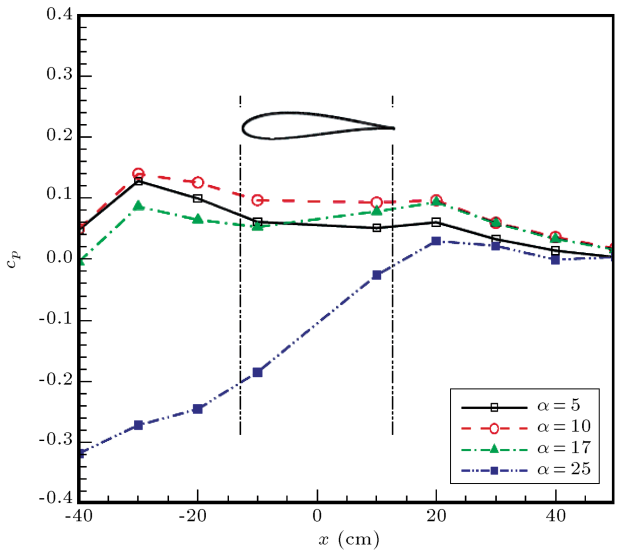

Figure 3. Pressure distribution on the bottom wall for the static model at a Reynolds number of 5.0×10^5.

to the free stream static pressure is observed. However, for high angle of attack, $\alpha = 25^\circ$, a completely different behavior is seen. Note that the static stall angle of attack for this airfoil is measured to be 11° [11]. The stagnation point at the lower surface moves towards the trailing edge and gets closer to the test section bottom wall. The strong adverse pressure gradient on the bottom wall, both upstream and under the model, may then be considered to be due to the proximity of the stagnation point. Also, the separated flow on the airfoil upper surface at this angle of attack affects the entire field, and the pressure increase at the bottom wall can be partly due to this phenomenon.

Note that at about a half chord downstream of the airfoil, the wall pressure for all angles of attack starts to converge to the free stream value, regardless of the model angle of attack. Even for $\alpha = 25^\circ$, where extensive separated flow regions exist downstream, the points of convergence of pressure are nearly the same as those for the lower angles of attack.

3.2. Dynamic results

Figure 4 shows the impact of the model dynamic motion on the unsteady wind tunnel wall pressure distribution at different times, corresponding to various model instantaneous angles of attack. The oscillation amplitude was $\pm5^\circ$. The location of the model in the test section, with respect to pressure ports, is shown on the top of each figure for convenience. For a 2 degree angle of attack during an upstroke motion, the effective angle of attack of the model decreases and the vertical clearance between the stagnation point on the model and the test section floor increases. As a result, the pressure on the floor under the model decreases, Figure 4(a).

For $\alpha(t) = 7^\circ$, the flow starts to separate from the body somewhere on the upper surface. During upstroke motion, the flow separation is delayed until higher angles of attack and the effective angle of attack decreases. However, due to the earlier time history of pressure, the wall pressure increases, compared to that in the static case. This emphasizes the importance of flow separation and its influence on the upstream region under the model. During downstroke motion, the width of the separated flow region increases, i.e., the flow remains separated until the angle of attack is reduced well below its static value. It seems that flow separation effects accumulate in the pressure time history, and this effect, at $\alpha(t) = 7^\circ$ for downstroke motion, reduces the pressure at the lower wall under the model. From Figure 4(a), the contribution of the flow separation is to add a time delay to the flowfield.

According to Figure 4(b), by increasing the reduced frequency, the motion time history becomes longer and the flowfield leads the motion [17]. Consequently, the wall pressure for both upstroke and

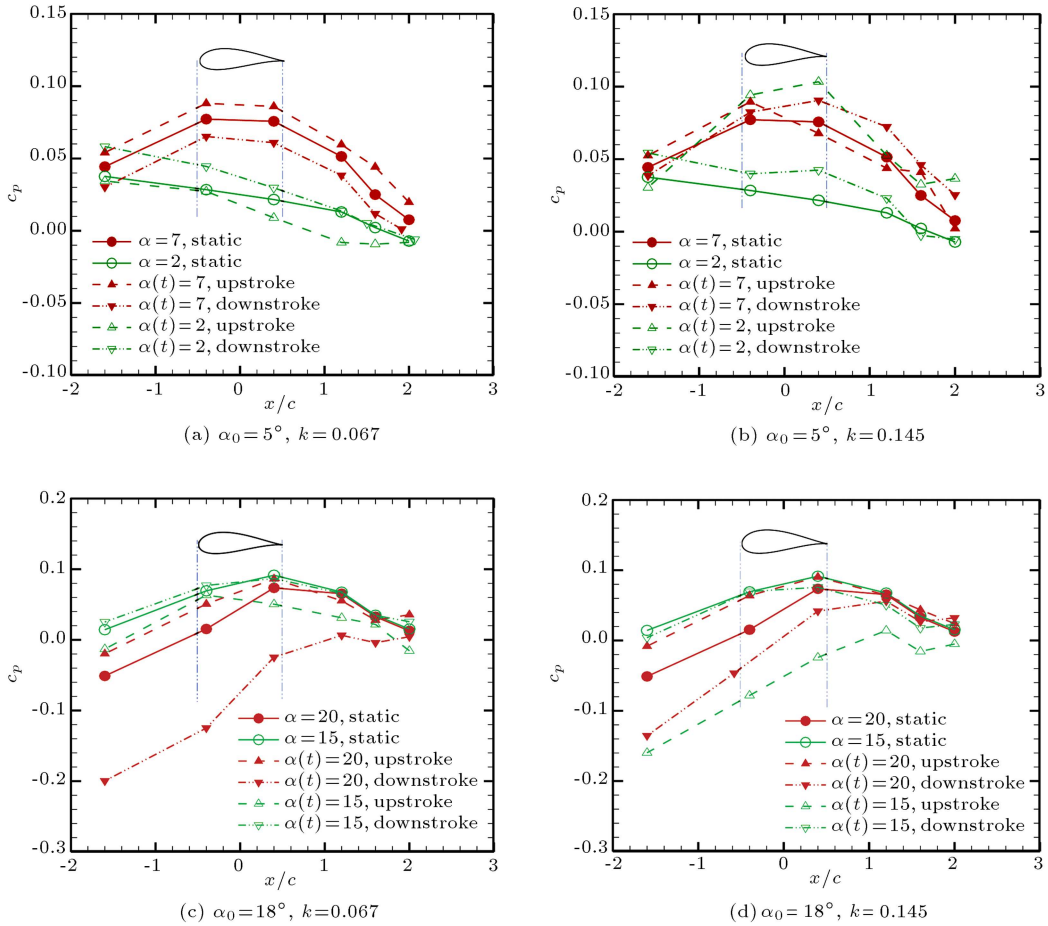

(a) $\alpha_0 = 5°$, $k = 0.067$ (b) $\alpha_0 = 5°$, $k = 0.145$

(c) $\alpha_0 = 18°$, $k = 0.067$ (d) $\alpha_0 = 18°$, $k = 0.145$

Figure 4. Pressure distribution on the bottom wall for the pitching model; oscillation amplitude: ±5°, Reynolds number: 5.0×10^5: (a) Mean angle of attack = 5°, reduced frequency = 0.067; (b) mean angle of attack = 5°, reduced frequency = 0.145; (c) mean angle of attack = 18°, reduced frequency = 0.067; and (d) mean angle of attack = 18°, reduced frequency = 0.145.

downstroke motion is higher than for the corresponding static cases.

For $\alpha(t) = 15°$, the airfoil is in a stall region. During upstroke motion, the effective angle of attack decreases and the stagnation point moves forward towards the leading edge. Thus, wall pressure under the model has been slightly decreased, compared to the static case.

For $\alpha(t) = 18°$, the airfoil is in the post-stall region. For dynamic motion, with amplitude of ±5° and mean angle of 15°, as shown in Figure 4(c), the flowfield experiences several important phenomena corresponding to pre stall, stall and post stall regions, as the model oscillates in the test section, for one oscillation cycle. These phenomena affect the pressure time history and, consequently, floor pressure for both upstroke and downstroke motion increases compared to that in the static case. One of the most important phenomena occurring for this case is the formation and shedding of the leading edge or stall vortex, which forms when the model is oscillating beyond the static stall angle. Once this vortex leaves the airfoil trailing edge, its effects can clearly be visible on the wall pressure distribution.

Further, note that for a mean angle of attack, 18°, the flow is completely separated from the airfoil upper surface. As stated earlier, the static stall angle for this airfoil is about 11°. The model lower surface and the test section lower wall form a convergent duct for the flow, within which, the subsonic flow accelerates and its pressure decreases. During downstroke motion, since the effective angle of attack increases, this venturi effect is stronger, and pressure decreases more than during upstroke motion.

The same discussion holds for higher reduced frequency, as shown in Figure 4(d). However, because of the longer pressure time history and an increase in the moving wall effects [18], the difference between wall pressure during upstroke and downstroke increases.

For a mean angle of attack of 18 degrees, Figure 4(c) and (d), for both reduced frequencies and both angles of 15 and 20 degrees, the wall pressure gradient just behind the airfoil, in downstroke motion, is higher, and, in upstroke, is smaller, than in the corresponding

static cases. This phenomenon, which is due to higher effective angle of attack during downstroke and lower effective a in upstroke, clearly represents the effects of the separated flow from the airfoil upper surface and its convection to the region behind the airfoil on the test section floor.

Figure 5 shows the pressure time histories for two mean angles of attack of 5 and 18 degrees at three locations on the bottom wall: point 7 under the model near the leading edge, point 6 under the model near the trailing edge, and point 4 downstream in the wake of the model.

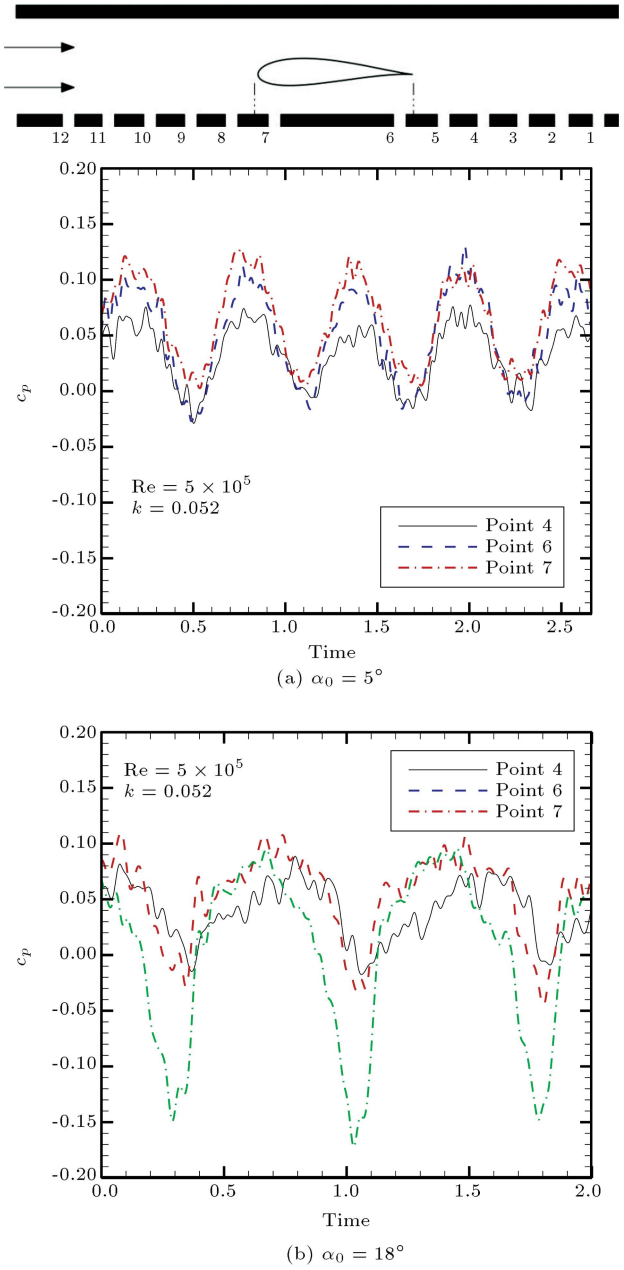

Figure 5. Pressure time history at different locations on the floor: (a) Mean angle of attack = 5°; and (b) mean angle of attack = 18°.

At lower mean angles of attack, Figure 5(a), the pressure time histories for the three points considered are nearly in-phase, in the sense that their maximum and minimum values occur nearly at the same times. The value of the pressure for the points under the model is also higher than the one located downstream in the wake. This is due to the high pressure region of the lower surface of the airfoil at $\alpha = 5°$, which has affected the pressure tabs on the bottom wall under the airfoil. Further, the pressure time history for the points under the airfoil at this angle of attack is nearly in phase with that located downstream. However, at 18 degree angle of attack, Figure 5(b), a phase shift is clearly observed between the pressure data for point 4 and those for points 6 and 7. This suggests that at low angles of attack, where the weak wake effect nearly diminishes downstream at point 4, the disturbances propagate nearly similarly in both streamwise and transverse directions, while, at high angles of attack, the phase difference between point 4 and those of points 6 and 7 is believed to be due to the strong vortices shed into the wake region of the airfoil downstream at point 4.

This phenomenon may better be observed from Figure 6, where the power spectrums for the pressure time histories are presented in the frequency domain. According to Figure 6(a), at low angles of attack, the power spectrums of the pressure fluctuations for both points 6 and 7 are nearly the same, indicating a similar convection mechanism for the disturbances from the airfoil to either of the two points. Further, point 10, located far upstream, receives minimum disturbances from the model fluctuations, as is expected. This picture is totally reversed at high angles of attack. According to Figure 6(b), at an angle of attack of 18 degrees, the upstream flow at point 10 is highly influenced by model oscillations, while there is no significant effect at point 4 downstream in the wake region. This confirms the former discussion on the diffusive role of the strong vortices shed into the wake region. In fact, the disturbances in the flow, due to the model oscillations, are nearly damped out far downstream. This can be seen from the low pressure power spectrum at point 4 and the high one at point 10. Note that points 6 and 7, which had nearly the same spectrums at low angles of attack, are shown to be different at $\alpha = 18°$ 7 and 10 are the neighboring points and have nearly the same value and behavior, while points 4 and 6, having similar spectrums, are located in the rear part of the test section, where the wake effects are dominant. As a result, the frequency jumps in the power spectrums, for both points 4 and 6, are weaker than the others. Thus, at low angles of attack, the mechanism for disturbance convection around the oscillating model is nearly the same in all directions, while at high angles of attack, the rear part of the test section, including the region under the trailing edge

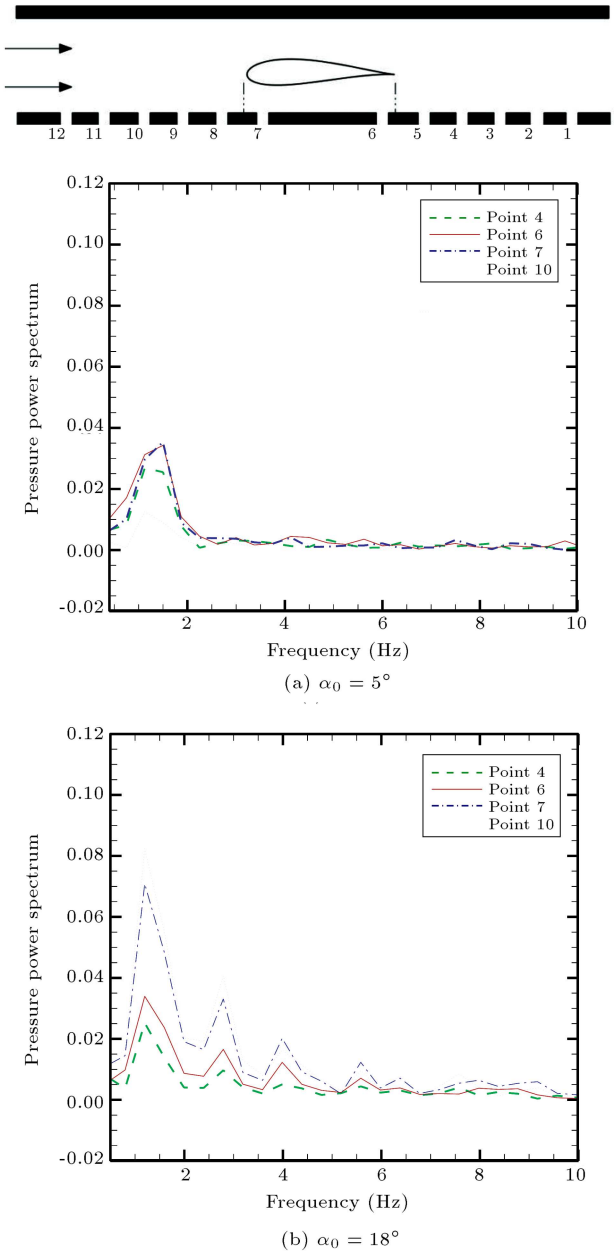

Figure 6. Pressure power spectrum at different locations on the floor; reduced frequency = 0.052, Reynolds number $= 5 \times 10^5$: (a) Mean angle of attack = 5°; and (b) mean angle of attack = 18°.

and downstream, experiences a different effect to that in the front region, near the leading edge and upstream.

Figure 7 shows the effects of mean angle of attack on the pressure time history for points 3 far downstream, 6 under the model near the trailing edge, 7 under the model near the leading edge and, finally, point 10 far upstream, all located on the test section floor.

For points 3 and 6 at the rear part of the test section, a slight phase shift is observed in the minimum and maximum pressure peaks, when the angle of attack changes. This phase shift is not observed at points 7 and 10 located in the front part of the test section, which is an indication of the wake effects. Further, note that the amplitude of the pressure fluctuations for point 3 is lower than the other points because of the wake dissipation effects discussed earlier.

Comparing Figure 7(c) and (d) with Figure 7(a) and (b), the sensitivity of the instantaneous pressure to the mean angle of attack is more pronounced for points 7 and 10 located in the front part of the test section than those in the rear part. It seems that the high pressure region under the model at high angles of attack, affects upstream more than downstream regions.

The pressure power spectrum shown in Figure 6 confirms the sensitivity of points 7 and 10 to the angle of attack changes. This is evident from the increased number of oscillatory modes in the power spectrums at these two points for a mean angle of attack of 18°.

Figure 8 shows the Reynolds number effects on the pressure power spectrums of points 2, 3 and 4 at both low and high angles of attack. According to Figure 8(a) and (b), increasing Reynolds number at a mean angle of attack of 5° diminishes some of the oscillatory modes in the flow, and the power spectrum at higher Reynolds number becomes smoother. The same behavior is observed for a mean angle of 18°, as shown in Figure 8(c) and (d). This suggests that for points 2, 3 and 4 in the wake region, viscous effects play a vital role in convecting the fluctuations arising from model oscillations downstream. Also, at high Reynolds numbers, some of these fluctuating modes have been eliminated from the pressure power spectrums at these points.

Further, note that when comparing Figure 8(a) with (c) and Figure 8(b) with (d), as the mean angle of attack increases, the values of the frequency peaks decrease, which means that the fluctuations generated by the model oscillations, once convected to the wake region, have been weakened when the model is set to a high mean angle of attack.

Figure 9 illustrates the same effect for point 7 located under the model near the leading edge, i.e., in the front part of the test section. Reducing the number of oscillatory modes at higher Reynolds numbers suggests that the viscous effects are not only responsible for convecting the fluctuations associated with the model oscillation to the wake region, but also the upstream influence of these fluctuations are due to viscous effects.

However, the effects of mean angle of attack on the values of the frequency peaks in the power spectrum are different for the upstream point in Figure 9 and the downstream ones shown in Figure 8. For point 7, as the mean angle of attack increases, the power spectrum is clearly increased, while, for points 2, 3 and 4 downstream in the wake region, the frequency peaks

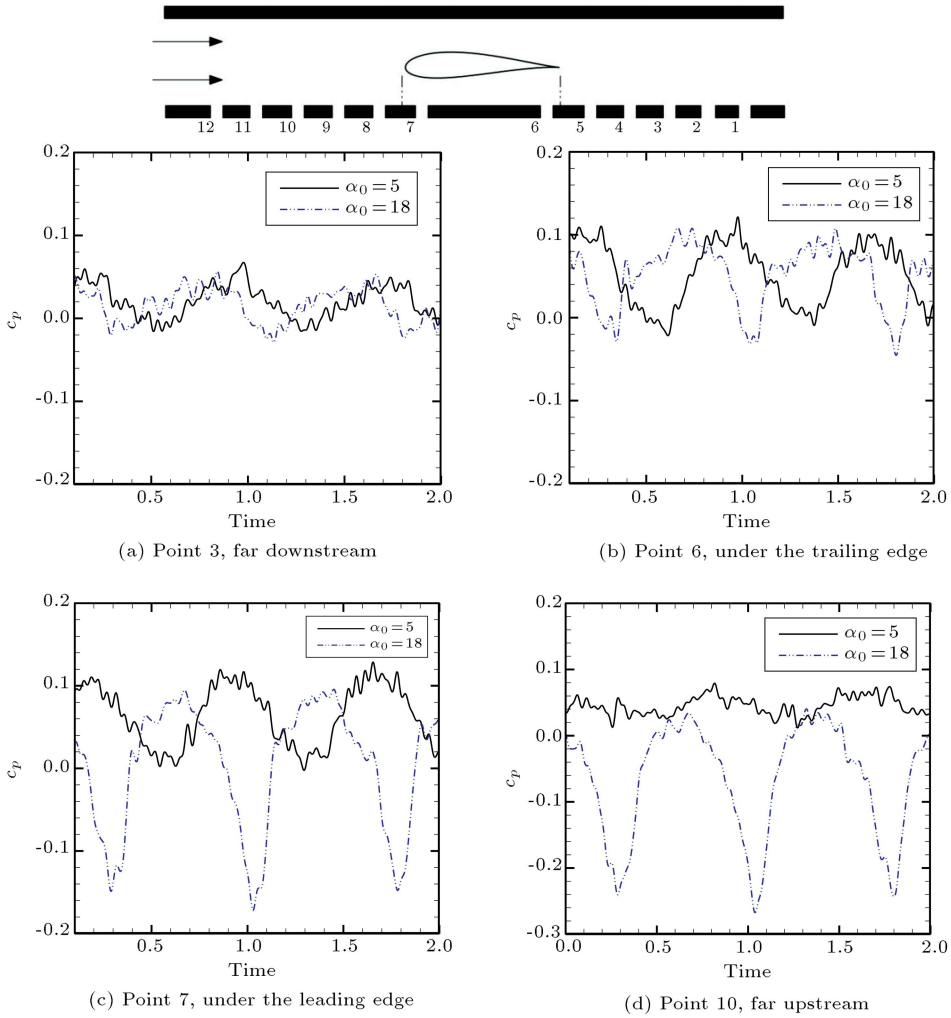

Figure 7. Effects of mean angle of attack on pressure time histories at different locations; reduced frequency = 0.052, Reynolds number: 5×10^5: (a) Point 3, far downstream; (b) point 6, under the trailing edge; (c) point 7, under the leading edge; and (d) point 10, far upstream.

in their power spectrum decrease, as the mean angle of attack increases.

The strong vortices shed in the wake region at high angles of attack may have attenuated the disturbances associated with model oscillations, while, in the upstream region, the high pressure flow, blocked by the wing lower surface, seems to amplify these fluctuations.

Time lag in the flowfield is one of the most important consequences of the unsteady motion of a model. The hysteresis loop in the aerodynamic parameters versus the instantaneous angles of attack of the model in an oscillatory motion is formed due to different flow patterns in upstroke and downstroke motions. These hysteresis loops have been previously observed in aerodynamic forces and moments, as well as in local pressure distribution on the model [13].

Figure 10 shows the aforementioned phenomena on the wind tunnel wall resulting from model oscillations, in a new way, in terms of hysteresis loops of wall pressure versus instantaneous angle of attack.

Shown in Figure 10 is the effect of mean angle of attack on the hysteresis loops of the wall pressures at points 3 and 6 in the rear part of the test section (downstream), and points 7 and 10 in the front part (upstream).

Generally speaking, the width of the hysteresis loops for all points shown increases, as increasing the mean angle of attack. This increase in loop width is an indication of a larger time lag in the unsteady flowfield between the up and down stroke motions. Note that for a mean angle of 5 degrees, with amplitude of $\pm 5^\circ$, the airfoil oscillates well below stall with a nearly linear aerodynamic behavior, while, for a mean angle of 18°, the airfoil oscillates in the post stall region, in which, the dynamic stall condition dominates.

Examining Figure 10, the changes in the width of the hysteresis loops for the upstream points are more pronounced than downstream ones, i.e., the increase in time lag when the model oscillates at higher mean angles is not felt in the downstream region as well as

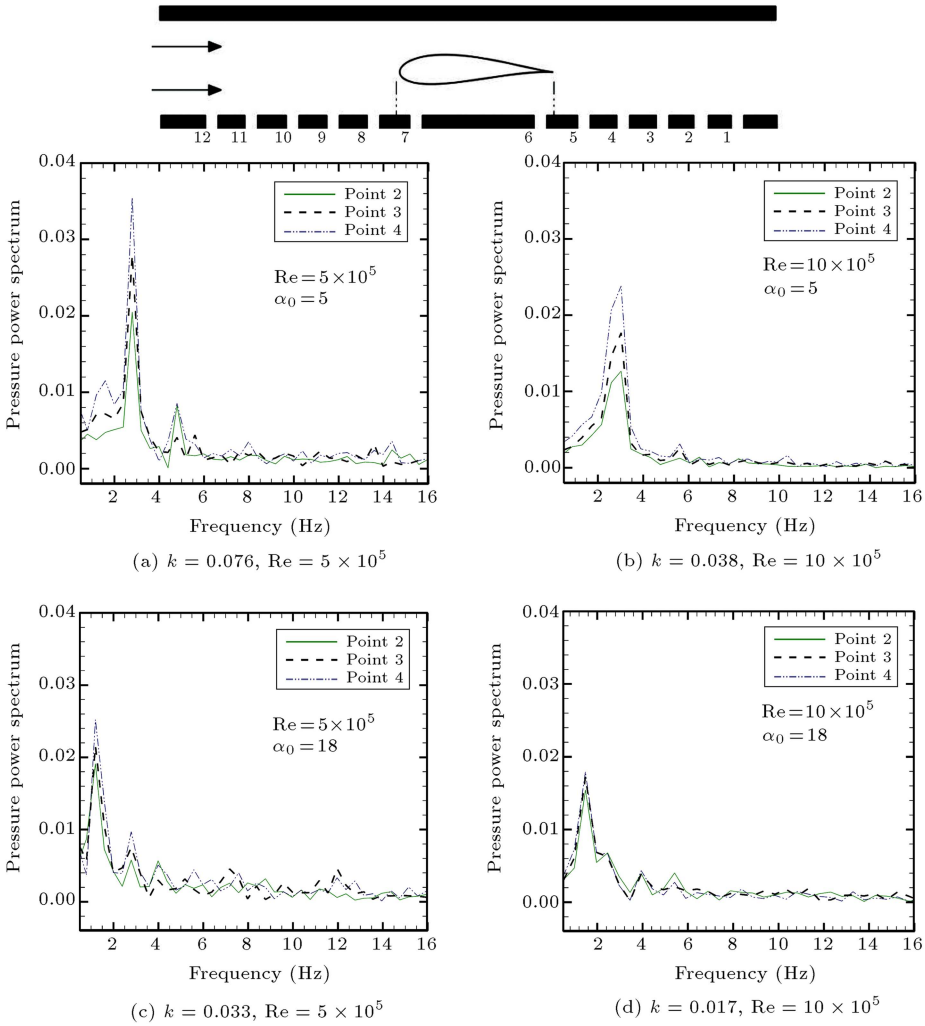

(a) $k = 0.076$, Re $= 5 \times 10^5$ (b) $k = 0.038$, Re $= 10 \times 10^5$

(c) $k = 0.033$, Re $= 5 \times 10^5$ (d) $k = 0.017$, Re $= 10 \times 10^5$

Figure 8. Effects of the Reynolds number on pressure power spectrum of the downstream points: (a) Reduced frequency = 0.076, Reynolds number = 5×10^5; (b) reduced frequency = 0.038, Reynolds number = 10×10^5; (c) reduced frequency = 0.033, Reynolds number = 5×10^5; and (d) reduced frequency = 0.017, Reynolds number = 10×10^5.

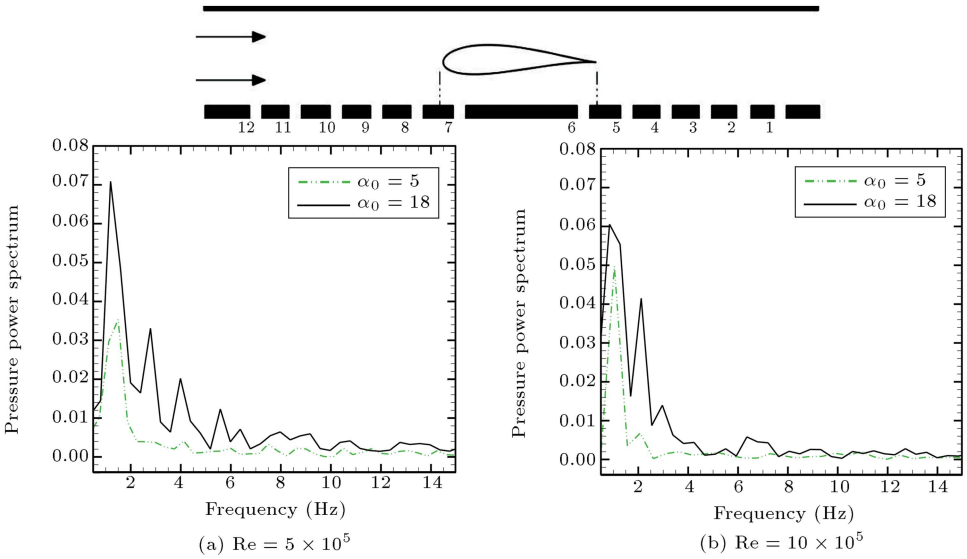

(a) Re $= 5 \times 10^5$ (b) Re $= 10 \times 10^5$

Figure 9. Effects of the Reynolds number on the pressure power spectrum at point 7 located upstream; reduced frequency =0.015: (a) Reynolds number = 5×10^5; and (b) Reynolds number = 10×10^5.

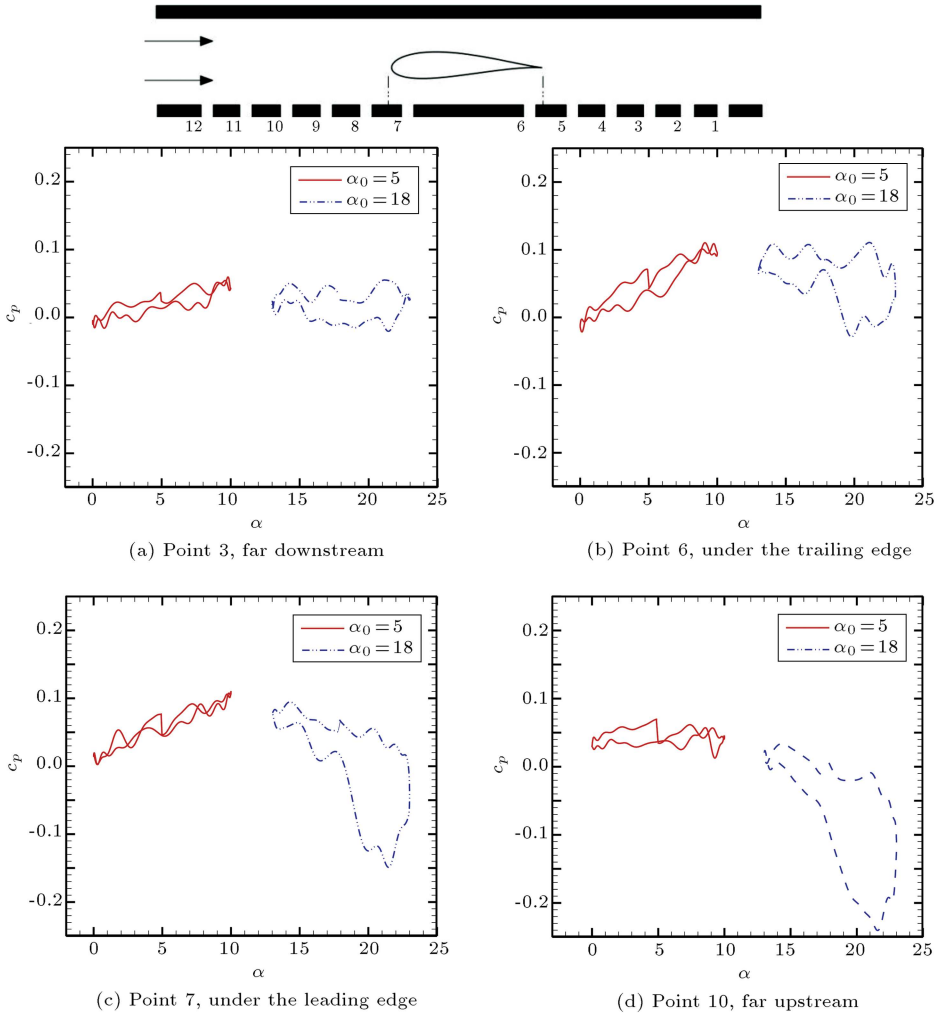

Figure 10. Variations of the wall pressures with model instantaneous angle of attack: (a) Point 3, far downstream; (b) point 6, under the trailing edge; (c) point 7, under the leading edge; and (d) point 10, far upstream.

that sensed in the upstream. This implies that the downstream flowfield receives less effect from model oscillations than that of the upstream, which may underscore the dominant role of stall vortices and the separated flows in the wake region, in comparison with the impact of fluctuations caused by model oscillations.

The width of hysteresis loops for the downstream points are also of the same order, while, for the upstream, the loop width at $\alpha = 18°$ is much larger, with a wider range of c_p. With the latter, it means that the value of pressure at the beginning of an oscillatory motion (one end) is much different from that at the end of the oscillation (the other end).

As stated earlier, the wake vortices, especially at high angles of attack, play an important role and can diminish the signature of fluctuations caused by model oscillations in the downstream region. For this reason, the hysteresis loops for the points located in the wake, as in Figure 10(a) and (b), are nearly of the same range, regardless of their mean angles of attack, while, for the upstream points, there is a remarkable difference between the pressure range in the hysteresis loop at both low and high angles of attack.

4. Conclusion

A series of wind tunnel wall pressure measurements was conducted in a low speed subsonic flow, to investigate the effects of the oscillations of an airfoil on the floor wall pressure signature at various locations.

According to the results, as model oscillation parameters change, wall pressure at points located in the front part of the test section in the upstream region exhibits a different behavior from that in the downstream part, especially at high angles of attack. This indicates that viscous effects play a vital role in convecting fluctuations arising from model oscillations downstream, and, as Reynolds number increases, these fluctuations will be attenuated. In other words, viscosity propagates fluctuations associated with the consequences of the pure dynamic motion of the model

to downstream. As the viscous effects decrease, most fluctuations felt in the downstream are those due to the static wake of the model, and are independent of model motion parameters such as reduced frequency and mean angle of attack. The results show that viscous effects are not only responsible for convecting fluctuations associated with the model oscillation downstream, but also have a remarkable effect on the upstream flow field.

Nomenclature

a	Angle of attack in static tests
α_0	Mean angle of attack in dynamic tests
α_A	Oscillation amplitude in dynamic tests
c	Chord length
Re	Reynolds number based on chord length
$k = \pi fc/V_\infty$	Reduced frequency
$c_p = \frac{p - p_\infty}{\frac{1}{2}\rho_\infty V_\infty^2}$	Pressure coefficient
p_∞	Free stream static pressure
p	Local static pressure on the wall

References

1. Beyers, M.E. and Ericsson, L.E. "Ground facility interference on aircraft configurations with separated flow", *Journal of Aircraft*, **30**(5), pp. 682-688 (1993).
2. Beyers, M.E. "Unsteady wind tunnel interference in aircraft dynamic experiments", *Journal of Aircraft*, **29**(6), pp. 1122-1129 (1992).
3. Kemp, W.B, Jr., *The Transonic Wind-Tunnel Wall Interference in High Reynolds Number Research*, Hampton, Virginia, Oct. 27-28, NASA CP-2009 (1976).
4. McCroskey, W.J., *A Critical Assessment of Wind Tunnel Results for the NACA 0012 Airfoil*, NASA TM-100019, NASA Ames Research Center (1987).
5. Fromme, J.A. and Golberg, M.A., *Two Dimensional Aerodynamic Interference Effects on Oscillating Airfoils with Flaps in Ventilated Wind Tunnels*, NASA CR- 3210 (1979).
6. Fromme, J.A. and Golberg, M.A. "Aerodynamic interference effects on oscillating airfoils with controls in ventilated wind tunnels", *AIAA Journal*, **18**(4), pp. 417-426 (1980).
7. Ahmed, M.R., Takasaki, T. and Kuhama, Y. "Aerodynamics of a NACA4412 airfoil in ground effect", *AIAA Journal*, **45**(1), pp. 37-47 (2007).
8. Duraisamy, K., McCroskey, W.J. and Baeder, J.D. "Analysis of wind tunnel wall interference effects on subsonic unsteady airfoil flows", *Journal of Aircraft*, **44**(5), September-October 2007, pp. 1683-1690 (Sept.-Oct. 2007).
9. Ericsson, L.E. and Beyers, M.E. "Aspects of ground facility interference on leading edge vortex breakdown", *Journal of Aircraft*, **38**(2), pp. 310-313 (2001).
10. Soltani, M.R., Bakhshalipour, A. and Seddighi, M. "Effect of amplitude and mean angle of attack on the unsteady surface pressure of a pitching airfoil", *Journal of Aerospace Science and Technology*, **2**(4), pp. 9-26 (December 2005).
11. Soltani, M.R. and Birjandi, A.H. "Effect of surface contamination on the performance of a section of a wind turbine blade", *AIAA*, paper 2007-1081 (2007).
12. Soltani, M.R. and Rasi, F. "Effects of plunging motion on the performance of a wind turbine blade section", *The Aeronautical Journal*, **111**(1123), pp. 571-587 (2007).
13. Soltani, M.R., Seddighi, M. and Rasi, F. "Comparison of pitching and plunging effects on the surface pressure variation of a wind turbine blade section", *Journal of Wind Energy*, **12**(3), pp. 213-239 (April 2009). DOI: 10.1002/we.286
14. Soltani, M.R., Rasi, F., Seddighi, M. and Bakhshalipour, A. "An experimental investigation of time lag in pressure measuring system", *Ankara International Aerospace Conference*, Turkey (2005).
15. Rae, H.W., Jr. and Pope, A., *Low-Speed Wind Tunnel Testing*, John Wiley & Sons, Inc. (1984).
16. Thomas, G.B., Roy, D.M. and John, H.L.V., *Mechanical Measurements*, Addison-Wesley, Publishing Company (1993).
17. Theodorsen, T. "General theory of aerodynamic instability and the mechanism of flutter", NACA Report 496 (1935).
18. Ericsson, L.E. and Beyers, M.E "Universality of the moving wall effect", *Journal of Aircraft*, **37**(3), pp. 508-513 (2000).

Biographies

Ali Reza Davari received his PhD degree in Aerospace Engineering from Sharif University of Technology, Tehran, Iran, in 2006, and is currently faculty member in the Department of Mechanical and Aerospace Engineering at the Science and Research Branch, Azad University, Iran. His research interests encompass experimental and applied aerodynamics, including new prediction and optimization methods and tools in aerodynamics, such as neural networks, DOE/RSM and evolutionary algorithms.

Mohammad Reza Soltani obtained his PhD degree in Aerodynamics from the University of Illinois at Urbana-Champaign, USA, in 1991, and is currently Professor in the Aerospace Engineering Department at Sharif University of Technology, Tehran, Iran. His research interests include unsteady and applied aerodynamics, design and building of wind tunnels and wind turbines, design, building and implementation of wind tunnel instruments, and measurement methods. He haspublished over 27 journals and 50 conference papers in his areas of research.

Mohsen Ghaeminasab obtained a BS degree in Aerospace Engineering from the Science and Research Branch of Azad University, Iran. His research interests include low speed wind tunnel testing and wind tunnel design. He has also experience in hot wire systems and both software and hardware elements design.